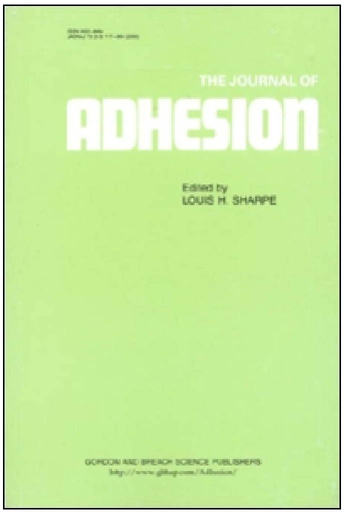

The Journal of Adhesion
Publication details, including instructions for authors and subscription information:
http://www.informaworld.com/smpp/title~content=t713453635

Finite Element Modeling of Double Lap Wood Joints

A. G. Zink[a]; R. W. Davidson[b]; R. B. Hanna[c]
[a] Department of Wood Science and Forest Products, Virginia Polytechnic Institute and State University, Blacksburg, Virginia, USA [b] Wood Products Engineering, State University of New York, Syracuse, NY, USA [c] Center for Ultrastructure Studies, State University of New York-College of Environmental Science & Forestry, Syracuse, New York, USA

To cite this Article Zink, A. G. , Davidson, R. W. and Hanna, R. B.(1996) 'Finite Element Modeling of Double Lap Wood Joints', The Journal of Adhesion, 56: 1, 217 — 228
To link to this Article: DOI: 10.1080/00218469608010509
URL: http://dx.doi.org/10.1080/00218469608010509

J. Adhesion, 1996, Vol. 56, pp. 217–228
Reprints available directly from the publisher
Photocopying permitted by license only

Finite Element Modeling of Double Lap Wood Joints

A. G. ZINK

Department of Wood Science and Forest Products, Virginia Polytechnic Institute and State University, Blacksburg, Virginia 24061-0323, USA

R. W. DAVIDSON

Wood Products Engineering, State University of New York, Syracuse, NY 13210, USA

R. B. HANNA

Center for Ultrastructure Studies, State University of New York-College of Environmental Science & Forestry, Syracuse, New York 13210, USA

(Received August 11, 1995; in final form December 4, 1995)

A general finite element model of a structural wood/adhesive connection was developed in this study and experimentally verified using a white light speckle technique. A bond link approach was developed and investigated to represent the adhesive connection.

A comparison of the stress distributions obtained with the model and those recorded experimentally revealed very closé agreement between the two techniques. Because the assumptions and results of the finite element model were verified with experimental evidence, it could be used to determine any number of geometric and material properties. In this study, the model was used to determine the influence of varying the overlap length on the distribution of normal and shear stresses. For the wood adherends used in this study, it was found that the distribution of stress was non-uniform but became more uniform with increasing overlapped regions.

KEY WORDS: Wood/adhesive connections; finite element modeling; double lap joint; computer vision; stress distribution; image analysis.

INTRODUCTION

When the common overlap joint is loaded in tension or compression, the stress distribution is very non-uniform. Stress concentrations often occur at the ends of the overlap that are significantly higher than the average stress along the glueline. The purported effect of the nonuniformity of the stress distributions has appeared as a possible explanation for characteristic types of failure and reductions in expected strength. Yet the analytical techniques to date are very limited in their application to double overlap wood connections because the assumptions in the models often do not apply to wood members, and there is even less experimental data. As a result, the objectives of this study were to develop a general finite element model of a double overlap wood joint, and to evaluate the model experimentally using the white light speckle technique for experimental mechanics.

BACKGROUND

Early Analytical Studies of Lap Joints

One of the earliest analyses of lap joints of any kind was a theoretical analysis by Volkerson[1] in 1938 on double lap joints. His analysis treated only the stress arising from the differential strain in the lap joints and did not examine the tension stress resulting from bending of the adherends. In his study, it was discovered that the distribution of stresses in a lap joint was not uniform. The highest stresses were shown to develop at either end of the overlap and the ratios of these peak stresses to mean stresses were influenced by the overlap length, the thickness of the adherends, the thickness of the adhesive layer, the stiffness of the adhesive, and the bending of the adherends. Goland and Reissner[2] extended Volkerson's analysis to include bending deformation of the adherends as well as transverse strains in the adhesive with the associated bending stresses. Although this analysis does include a few simplifications and approximations, it is to date one of the more rigorous mathematical studies of the stress distributions in single lap joints.

By a variation and extension of Goland and Reissner's method, Cornell[3] determined the distribution of stress in cemented metal lap joints using the assumption that the adherends behave like simple beams and the lower modulus adhesive layer can be represented by a number of shear and tension springs. Cornell developed a complicated set of differential equations to describe the transfer of load in one adherend through a spring system to the other adherend. With certain assumptions, this set of equations can be reduced to a pair of ordinary differential equations of the tenth order whose solutions are readily found. The mathematical analysis is fundamentally simple but the expressions involved are quite complicated. Cornell compared his theoretical calculations with the results of photoelastic and brittle lacquer experiments and found that his spring-beam analogy solution gives a fairly accurate picture of the distribution of stresses in lap joints.

There have been many studies conducted since the early work, but most of them rely on the basics as developed in Goland and Reissner[2]. In general, the results of the theoretical analyses to date indicate that the highest stresses develop at either end of the overlap and the ratios of these stresses to the mean stress (the concentration factor) are highly dependent on the overlap length. Complex or simple rigorous investigations using the theory of elasticity in general give the approximate highest stresses which result from the external loading for adherends and adhesives which are isotropic, elastic, and homogeneous. Wood is none of these. It is highly anisotropic, elastic only up to a point, and homogeneous only on a gross scale.

Thus the theoretical results found using isotropic analyses and materials can only serve as indicators of the expected distributions and strength. The stress concentrations predicted at the ends of the overlaps are very important in all structures, especially those joined by adhesive bonding. In theory, a sharp corner or crack causes an infinite stress concentration referred to as a singularity, which is impossible in reality. But it is in just these regions of maximum stress where failure is likely to be initiated that the assumed boundary conditions of the mathematical theories are least representative of reality.

Finite Element Modeling of Adhesive Connections

The finite element method is a well-established means for mathematically modeling stress problems. Its advantages lie in the fact that the stresses in a body of almost any geometrical shape and composition can be determined. As a result, the method is especially useful for analyzing adhesive connections. In this method, the structure of the continuum being analyzed is approximated as the assembly of discrete regions (elements) connected at a finite number of points (nodes). The resulting set of simulataneous equations is then solved with a computer. If sufficient boundary conditions are specified to guarantee a unique solution, the displacements at each node in the structure can be obtained. Once a finite element model has been developed and verified experimentally, it is a powerful tool that can be expanded and used in place of expensive and time-consuming experimentation.

A number of finite element investigations have been carried out on a wide range of adhesion problems. The only difficulty encountered with this approach is that modeling the glueline presents some problems. To overcome this difficulty some models have been used that model the bonded structure without taking special account of the glueline. Erdogan and Ratwani[4] have found that if the glue interface is not accounted for, the load transfer between the adherends occurs at the outer boundaries of the bond only, and this is not the case in continuous glue joints in reality.

Several modeling schemes have been published that do take into account the bonds of lap joints. Triangular or quadrilateral shaped two-dimensional plane stress or plane strain elements are most often used to model the adherends. Similar elements have been used to represent the adhesive component also[5-14]. Due to the geometry of gluelines, long thin elements are required for modeling and this results in very large aspect ratios for these elements. It has been established that an element tends to stiffen and lose accuracy as its aspect ratio increases[15]. Using two-dimensional planar elements to approximate the glueline necessarily makes the analysis mesh-dependent and may result in questionable accuracy in the region of the glueline.

An alternative considered by some is a special interface element to represent the adhesive connection[16-20]. Interface elements assume that the undisplaced nodes of one adherend are coincident with the corresponding nodes of the other adherend. While this approach creates an element of zero thickness, the thickness of the glueline is usually taken into account in the stiffness matrix of the element and the elastic properties of the adhesive are required. This method is also mesh-dependent and reliant on material properties that are difficult to obtain reliably. The resulting localized inaccuracies have a large effect on the stress distributions in the region of most interest, the glueline.

A special bond link element was developed in early finite element studies of reinforced concrete beams[21] that shows some promise for use with bonded joints. With this approach, the adhesive connection would be considered an elastic medium acting basically as tension and shear springs between the adherends. In a finite element model of a bonded joint, the adhesive connection would be conceptualized as a series of linear spring elements of zero dimension. The springs represent the stiffness of the connection. The forces in the springs give a measure of the bond stress distribution along the connection and the springs permit slippage to take place as the load is applied. The springs have no physical dimension and only the stiffnesses are used. With bond links, the model does take into account the adhesive connection, it is not mesh dependent, and it does not rely on properties that have been difficult to determine. This approach is based on the theory of elasticity and similar to that proposed by Cornell[3].

METHODS AND MATERIALS

A general finite element model was developed for analysis of double lap shear wood connections that could be used to determine the influence of any desired material or geometric parameter and then expanded to account for other factors such as time dependency. Yellow-poplar (*Liriodendron tulipifera*) was selected for experimental analysis because it glues very easily with a wide range of glues, under a wide range of gluing conditions and because the relative uniformity in anatomical structure would minimize variability in the results due to material inhomogeneities. The overlap lengths that were examined ranged from 12.7 mm to 44.5 mm in 6.35 mm increments (0.5″ to 1.75″). The dimensions represents a one-tenth scale of the overlap lengths used in timber wood truss and other mechanical connections. The side adherends were 50.8 mm (2″) long by 25.4mm (1″) in cross section. The center adherend was 89 mm (3.5″) long by 25.4 mm (1″) in cross section. The adhesive was a resorcinol-formaldehyde structural wood adhesive. Figure 1 is a diagram of the general double lap shear structural wood connections examined in this study.

Finite Element Model

The model developed for this study was a two-dimensional, plane stress finite element model. The model is linear elastic, considers only static in-plane loads, and assumes orthotropic, homogeneous material properties for the adherends. Two dimensional, 8-node, isoparametric quadratic quadilateral elements were used to represent the wood adherends. A quadratic function is used to formulate both the geometry and displacement field for this element and the displacements may be either linear or quadratic. The element formulation is based on the standard isoparametric approach and can be found in many textbooks on finite element modeling, for example Ref. 22. A graded mesh of elements was established that was fine near the gluelines and more coarse away from the gluelines. The coarse mesh furthest from the gluelines consisted of elements that were 1.59 mm (0.0625″) perpendicular to the gluelines and 6.35 mm (0.25″) in length, grading into elements that were 3.175 mm (0.125″) in length and 1.59 mm (0.625″) across. Elements near the gluelines were 1.59 mm (0.0625″) square. Figure 2 is an example of the element mesh used for the 12.7 mm (0.5″) overlap model. While the model geometry is symmetric about the centerline, the full model was analyzed rather

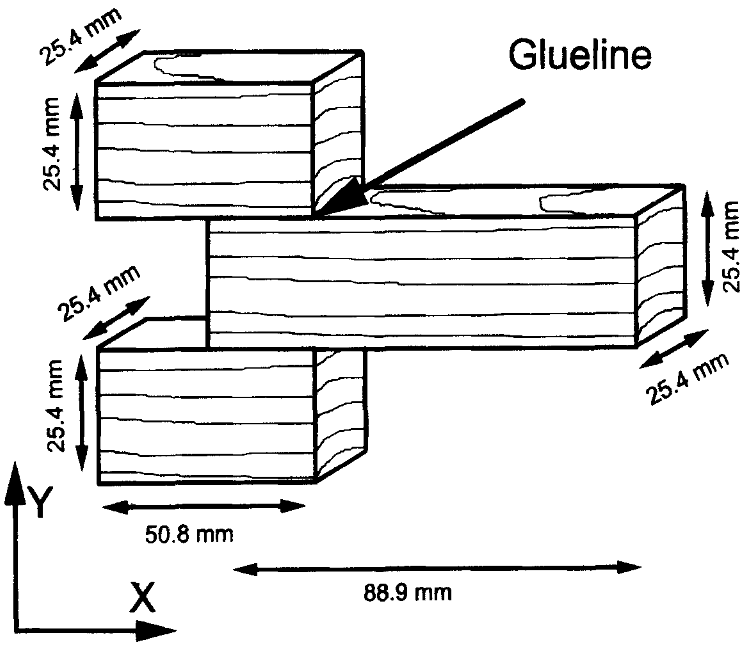

FIGURE 1 Diagram of general double lap shear structural wood connection.

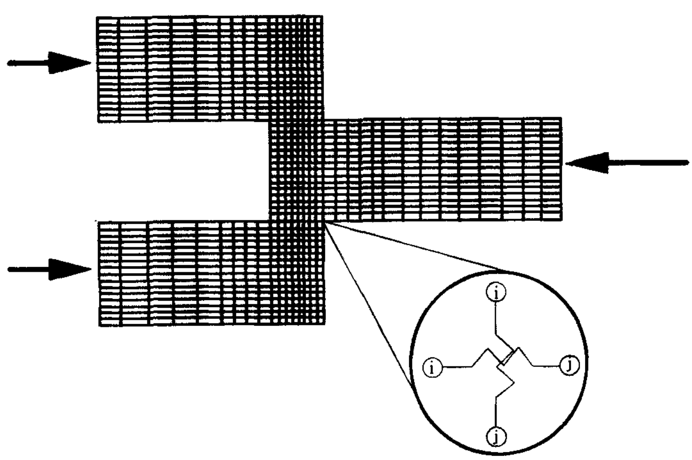

FIGURE 2 Example element mesh used for 12.7 mm overlap length specimen.

than taking advantage of the symmetry to allow for using dissimilar wood members as side adherends. Each species of wood used will process different mechanical properties and this must be taken into account in the full model if the side members are not the same type of wood.

The convergence requirements of the mesh were met by repeatedly analyzing the problem each time using a finer mesh of elements until no change was observed with further mesh refinement. The least number of adherend elements used was 912 for the shortest overlap model and the most was 1920 for the longest overlap model. A compression load was applied to displacement-coupled nodes of the non-bonded end of the center adherend as seen in Figure 2, and the support conditions prohibited any translation or rotation of the nodes at the free ends of the side adherends.

The adherend material properties required for this element were the modulus of elasticity parallel to the grain (E_L) the modulus of elasticity perpendicular to the grain (E_R), the shear modulus (G_{RL}) and Poisson's ratio (μ_{RL}). The average values for yellow-poplar test specimens at 9% moisture content were found to be: $E_L = 10.8$ GPa (1.57×10^6 psi), $E_R = 1.23$ GPa (1.87×10^5 psi), $\mu_{RL} = 0.35$ using ASTM D143-86 Standard Methods of Testing Small Clear Specimens of Timber[23]. The average shear modulus (G_{RL}) was derived using a mathematical expression that relates the shear modulus to the experimentally-measured values using Hooke's law, and was determined to be 0.869 GPa (1.26×10^5psi).

The adhesive connection was idealized as a series of spring elements of zero dimension (a linkage element). Linkage elements consisted of two linear spring elements placed at right angles to each other and located at the coincident corner nodes of the adherend elements, as seen in Figure 2. Each spring had one degree of freedom (translation in either x or y), and displacement of each degree of freedom was completely independent of the other. The springs transmitted shear and normal forces between the nodes and represent the shear and normal stiffness of the adhesive connection. The forces in the bond links give a measure of the bond stress distribution along the connection. The bond links permit a certain amount of slippage to take place as the load is applied, but no fracture or failure component is included in this analysis. To ensure inter-element compatibility along the gluelines, the midside nodes of the adherend elements were removed along the sides that were on the gluelines, thereby making all elements along the gluelines linear. The lap joint section of the model was zero thickness and the linkage elements were placed at the coincident adherend corner nodes along the overlapped region.

Because a high stiffness is generally experienced with good, rigid adhesive connections between wood and structural adhesives, a high stiffness connection is assumed in this study. This situation is most commonly modeled by assigning large stiffness values to each element in the linkage element[24–27]. The actual stiffness values used in this study were determined through an equivalent stiffness study. An equivalent stiffness approach is required because using values of the adhesive modulus of elasticity and shear modulus obtained from bulk specimens of adhesive does not adequately represent the actual stiffness of a structural wood connection[28–30]. With this approach, the values of the shear and normal stiffness of the adjacent wood elements are used as the initial trial values in the linkage elements along the overlap regions. The value of the maximum axial displacement in the wood-spring model is then compared with the maximum axial displacement in a solid-sawn wood model of exactly the same material and geometry. The comparison is made with a solid-sawn model beacuse it is assumed that the rigid-glued wood joint cannot exhibit displacement greater than that of solid wood. The displacements from the solid-sawn model are used to scale the glueline stiffness to values that converge to those of a rigid, stiff bonded connection. These stiffness values were found to be two orders of magnitude greater than the stiffness of the adjacent wood elements. The value used for the normal stiffness was 4.35×10^{12} kg/m (1.57×10^{8} lb/in) and for the shear stiffness 2.82×10^{12} kg/m (1.02×10^{8} lb/in) was used. By using the linkage element approach to model the adhesive connection, the model does take into account the gluelines and it is neither mesh-dependent nor material-dependent.

Experimental Evaluation

Distribution of strain along the gluelines was experimentally measured using the Digital Image Correlation Technique (DICT) as described in Zink *et al.*[31,32]. This is a white light speckle technique that utilizes mathematical correlation of digital images of the test specimen surfaces recorded during mechanical testing. A cross correlation of two functions is used to indicate the relative amount of shifting between the two functions for various degrees of displacement. In the case of experimental mechanics, the displacement imposed on the test specimens during mechanical loading is measured as the degree of shifting of the light intensity patterns as found by the cross correlation criterion. In this study, a bilinear interpolation of the gray levels between pixels was used to represent the continuous pattern on the specimen and sub-pixel accuracy was achieved to the level of 0.01 pixels. The correlation function used for minimization was a least squares correlation to measure how well the subsets match. A coarse-fine iterative procedure was employed for the searching algorithm. DICT has been employed to obtain quantities of interest in such fields as rigid body mechanics, dynamics, fluid mechanics, biomechanics, fracture mechanics, and micromechanics[33-39]. The technique has been applied to a vast range of loading, environmental and testing conditions, and materials.

RESULTS AND DISCUSSION

Comparison of Model and Experimental Values

While the finite element method has become a well-established method of analysis for problems that cannot be addressed by classical analyses, the computed results must be judged in some way or compared with expectations before the model can be used with certainity. To validate the assumptions and results and to verify the accuracy of the model, the distributions of normal and shear stress along the gluelines were compared with experimental evidence from ten test joints. Figure 3 is an example plot of shear stress along the gluelines obtained from the finite element model and experimental testing for the joints with 12.7 mm and 38.1 mm overlapped regions. Nine measurement points spaced 1.59 mm apart for the 12.7 mm overlap and 4.76 mm apart for the 38.1 mm overlap were used to evaluate the stress levels along and across the gluelines. The location of the measurement points on the test specimen images corresponded to the nodal point location along the gluelines in the finite element model (illustrated in

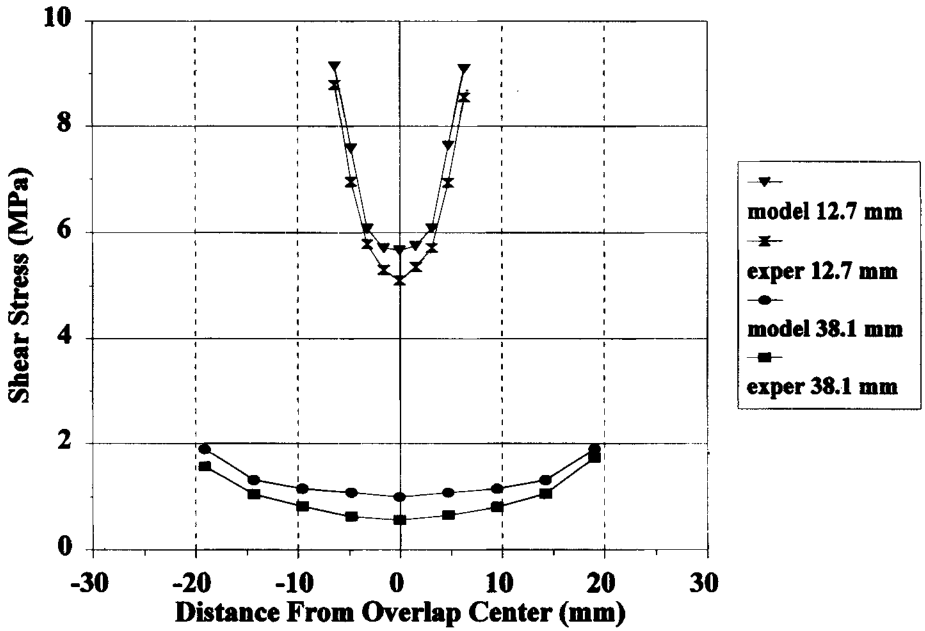

FIGURE 3 Comparison of shear stress obtained with the finite element model and the experimental test specimens for the 12.7 mm and 38.1 mm overlap length specimens.

Figure 2). The load level for this plot was 2260N. The strain values obtained from the experiments were converted to stresses using Hooke's Law which is the assumed constitutive relationship for wood stressed in the elastic region of the stress/strain behavior. The comparison is made at low load levels since the finite element model assumes linear, elastic behavior to failure, but wood is linear, elastic only for a portion of the loading process.

While the trends exhibited by the model and the test values for the shear stresses are identical, the experimentally–measured values indicate more variability in the distribution and lower values in general. Figure 4 is an example of the results of the comparison of normal stresses across the gluelines obtained with the model and the experiments on joints with 12.7 mm and 38.1 mm overlapped regions. Again, it is observed that the trends are similar but there are some slight differences in magnitude and variability. Deviation is greatest at the ends of the joints where the stress gradient is highest and is a result of assuming a rigid, stiff adhesive connection constructed with a very high modulus adhesive. Although the wood used for experimental verification was homogeneous in anatomical structure, the elastic properties do vary on a microscopic scale and some variability is expected. Within the scatter of the experimental data for the ten joints tested, the model results predict the stresses along the gluelines very well.

Model Distribution Along the Gluelines

Because the general model stress values compared very well with those obtained experimentally, it can be used to evaluate joints made with any desired species of wood,

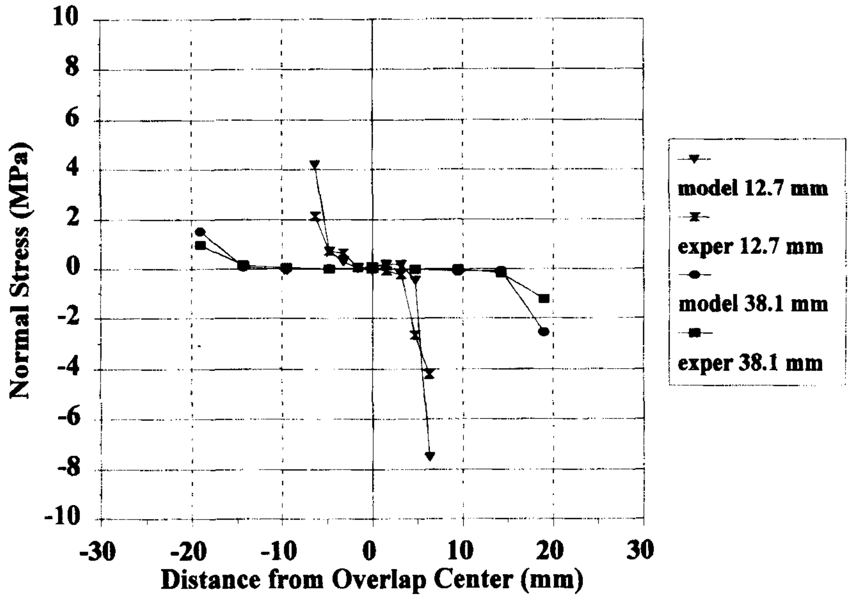

FIGURE 4 Comparison of normal stress obtained with the finite element model and the experimental test specimens for the 12.7 mm and 38.1 mm overlap length specimens.

non-identical adherends, other geometries or adhesive properties, and even joints with discontinuities in the gluelines or defects in the adherends. The influence of varying overlap lengths was investigated in this study to demonstrate the utility of this general model.

The distribution of normal and shear stress was determined using the adherend nodes located along a glueline. Due to the geometric symmetry, the distribution as approximated by the finite element model is identical in magnitude and shape for both gluelines and the stresses for only one gluline are presented. Figure 5 is a plot of the shear stresses obtained with the finite element model for the nodes along a glueline for a series of overlap lengths at a load level 1560 N. Examination of Figure 5 indicates that the distribution of shear stress along the overlapped region is not uniform even for the longest overlaps studied. Because the rigidity of the adhesive in the joints is not negligible in comparison to the wood members and the load and support reactions are not co-linear, the stress distribution in these structural wood connection is quite complex. The maximum values of shear stress occur at each end of the lap joint and the minimum occurs at the center of the joint. As the overlap length increases, the distribution becomes more uniform, but at a diminishing rate. For example, for an overlap length increase from 12.7 mm to 19.1 mm, the reduction in peak shear stress is 862 KPa but for the same 6.35 mm change from 38.1 mm to 44.5 mm in overlap length, the reduction in peak shear stress is only 172 KPa. With the longer overlapped regions, the load is transferred more uniformly and there is less stress concentration at the sharp, re-entrant corners at the joint ends.

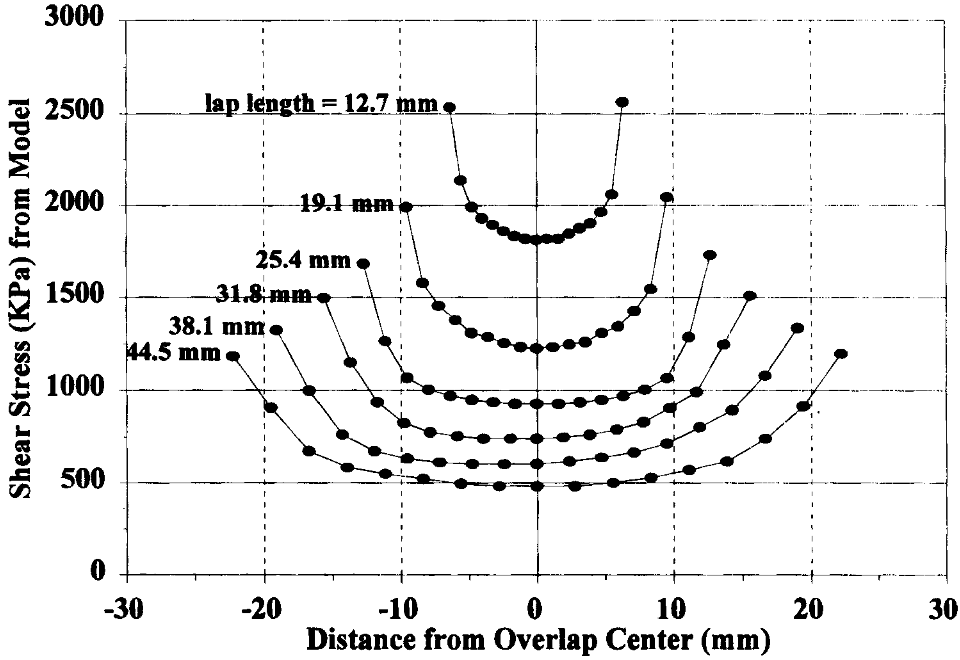

FIGURE 5 Shear stress obtained with the finite element model for a series of overlap lengths in double lap shear joints.

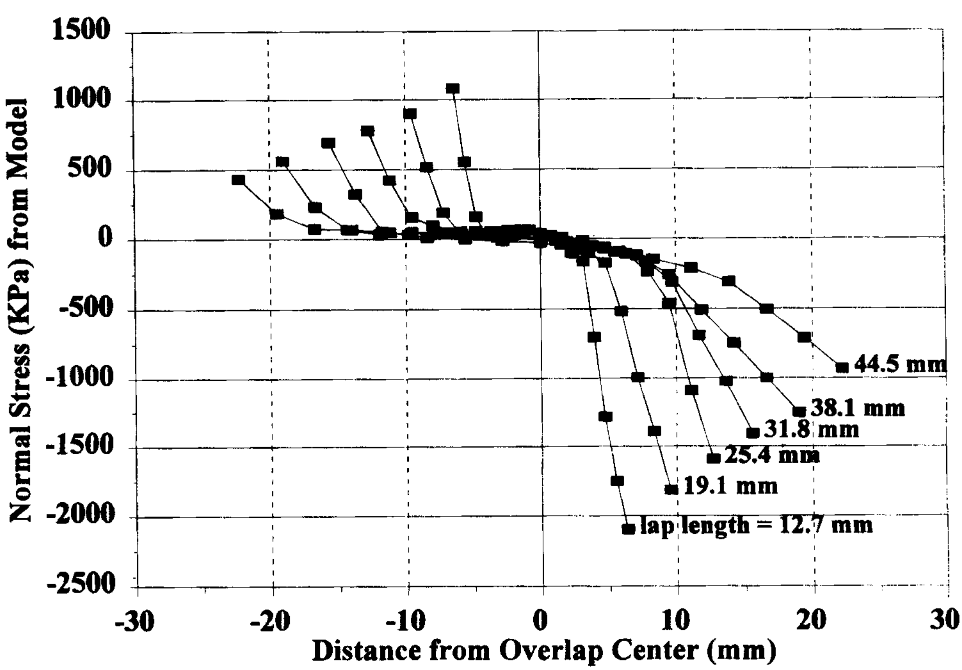

FIGURE 6 Normal stress obtained with the finite element model for a series of overlap lengths in double lap shear joints.

Figure 6 is a plot of the normal stresses across the glueline (σ_y) obtained with the general finite element model and varying overlap lengths at a load of 1560 N. The normal stress distribution is very non-uniform for all the overlap lengths in this study. Very high compression stresses are indicated on one end of the lap joint and tension stresses at the other end. These normal stresses across the glueline arise because the directions of the applied load and the reactions at the supports of the lap joint are not co-linear and there is a bending moment applied to the side members of the joint. The convex bending of the side adherends causes the compression at the loaded end of the center adherend and tension at the bonded end. As with the shear stress for increased overlapped regions, the normal stress distribution becomes more uniform along the length of the joint at a diminishing rate. The concentration of stress at each end of the overlapped region is reduced with an increase in overlap length.

SUMMARY AND CONCLUSIONS

A general finite element model of structural wood/adhesive connections was developed that utilized a bond link approach to model the adhesive connection. The bond link consisted of two orthogonal spring elements, one representing the shear stiffness and the other, the normal stiffness of the connection. With the bond links, the model does take into account the adhesive connection, the model is not mesh-dependent, and does not rely on properties that have been difficult to determine.

A comparison of the normal and shear stress distributions along and across the adhesive connection as determined with the finite element model and those obtained experimentally showed very close agreement. Once a finite element model has been verified with experimental evidence, it can be used in the place of costly and time-consuming experimentation. The utility of the model developed in this study was demonstrated by determining the influence of overlap length on the distribution and concentration of stress along the glueline. For the wood adherends used in this study, it was determined that the distribution of both normal and shear stresses was non-uniform and maximum values occurred at the ends of the overlapped regions. With increasing overlap length, both the normal and the shear stress distribution became more uniform and the concentration of stress at the corners of the joints was reduced.

Acknowledgements

The authors are grateful to Mr. Arnold C. Day and Mr. John McKeon, SUNY-CESF, Syracuse, New York, USA, to Dr. James A. Mandel, Syracuse University, and to the USDA CSRS McIntire-Stennis Forest Research Program for financial assistance.

References

1. O. Volkerson, *Luftfahrtforschung* **15**, 41–47 (1938).
2. M. Goland and E. Reissner, *J. Appl. Mech. Trans. ASME* **11**, A17–A27 (1944).
3. R. W. Cornell, *J. Appl. Mech. Trans. ASME* **17**, 335–364 (1953).
4. F. Erdogan and M. Ratwani, *J. Composite Materials* **5**, 378–393 (1971).
5. G. R. Wooley and D. R. Carver, *J. Aircraft* **8**(10), 817–820 (1971).

6. A. D. Crocombe and I. E. J. Evans, *J. Adhesion* **26**, 199–213 (1988).
7. R. J. Leichti, *Proceedings International Conference on Timber Engineering*, Seattle, WA, Vol 1 (1988), pp. 647–653.
8. V. Weissberg and M. Arcan, *Adhesively Bonded Joints; Testing, Analysis, and Design, ASTM STP 981* American Society for Testing and Materials, Philadelphia, PA, (1988), pp.28–38.
9. R. D. Adams, *J. Adhesion* **30**, 219–242 (1989).
10. L. H. Groom and R. J. Leichti, *J. Adhesion* **44**, 69–83 (1994).
11. J. Pascal, E. Darque-Ceretti, E. Felder and Pouchelon, *J. Adhesion Sci. Technol.* **8**(5), 553–573 (1994).
12. P. R. Borgmeier and K. L. DeVries, *J. Adhesion Sci. Technol.* 7(9), 967–986 (1993).
13. J. H. Choi and D. G. Lee, *J. Adhesion* **44**, 197–212 (1994).
14. R. D Adams and V. Mallick, *J. Adhesion* **38**, 199–217 (1992).
15. R. D. Cook, D. S. Malkus and M. E. Plesha, *Concepts and Applications of Finite Element Analysis* (John Wiley & Sons, New York, NY, 1989).
16. R. M. Barker and F. Hatt, *AIAA Journal* **11**(12), 1650–1654 (1973).
17. C. L. Johnson, *AIAA Journal* **27**(1), 79–86 (1989).
18. H. R. Milner and E. Yeoh, *J. Struct. Eng.* **117**(3), 755–766 (1991).
19. P. J. Pellicane, *Forest Prod. J.* **42**(1), 50–52 (1992).
20. R. E. Goodman, R. L. Taylor and T. L. Brekke, *J. Soil Mech. and Foundations Div. ASCE* **93**(SM3), 637–659 (1968).
21. D. Ngo and A. C. Scordelis, *ACI J.* March, 152–163 (1967).
22. O. C. Zienkiewicz and R. L. Taylor, *The Finite Element Method*, 4th Ed. (McGraw-Hill Book Company, New York, NY, 1989).
23. ASTM Standard D143–83 *Standard Methods of Testing Small Clear Specimens of Timber* (American Society for Testing and Materials, Philadelphia, PA, 1986).
24. *ANSYS Theoretical Manual* (Swanson Analysis Systems, Inc., Houston TX, 1972).
25. A. S. Kuo, *AIAA J.* **22**(10), 1460–1464 (1984).
26. M. E. M. El-sayed, *Computers & Structures* **33**(4), 977–981 (1989).
27. V. J. Borowski, R. L. Steury and J. L. Lubkin, *SAE Trans.* Paper 730506 (1973).
28. H. Wernersonn and P. J. Gustafsson, *Proceedings International Conference on Timber Engineering*, Seattle, WA, Vol. I, pp. 673–682 (1988).
29. W. T. Simpson and V. R. Soper, Res. Note FPL-0198, USDA Forest Service, Forest Products Laboratory, Madison, WI (1968).
30. D. Jangblad, P. Gradin and T. Stenström, *Adhesively Bonded Joints; Testing, Analysis, and Design, ASTM STP 981* American Society For Testing and Materials, Philadephia, PA, (1988), pp. 28–38.
31. A. G. Zink, R. W. Davidson and R. B. Hanna, *J. Adhesion* (in print).
32. A. G. Zink, R. W. Davidson, and R. B. Hanna, *Wood & Fiber Sci.* **27**,(4), 346–359, (1995).
33. M. A. Sutton, W. J. Wolters, W. H. Peters, W. F. Ranson, and S. R. McNeill, *Image and Vision Computing* **1**(3), 133–139, (1983).
34. W. H. Peters and W. F. Ranson, *Optical Engineering* **21**(3), 427–431, (1982).
35. Z. H. He,M. A. Sutton, W. R. Ranson and W. H. Peters, *Experimental Mechanics* **24**(2), 117–121, (1984).
36. W. F. Ranson, D. M. Waler, and J. B. Caulfield, "Computer Vision in Engineering Mechanics", a Discussion paper prepared for the NSF Workshop on Solid Mechanics Related to Paper, August, 1986, Blue Mountain Lake, N.Y.
37. P. F. Luo, Y. J Chao and M. A. Sutton, *Proceedings 1994 SEM Spring Conference on Experimental Mechanics*, Baltimore, MD pp. 248–253 (1994).
38. G. Vendroux "Scanning Tunneling Microscopy in Micromechanics Investigations", Ph.D. Thesis, California Institute of Technology, Pasadena, CA (1994).
39. D. Choi, J. L. Thorpe and R. B. Hanna, *Wood Sci. & Technol.* **25**, 251–262 (1991).